



Flexibility study for an MSF desalination plant

Enrique E. Tarifa^{a*}, Samuel Franco^a, Demetrio Humana^a, Sergio Mussati^b

^aUniversidad Nacional de Jujuy – CONICET, Gorriti 237, 4600 San Salvador de Jujuy, Argentina

Tel. +54 (388) 4221587; Fax +54 (388) 4221581; email: eetarifa@arnet.com.ar

^bINGAR – CONICET, Avellaneda 3657, 3000 Santa Fe, Argentina

Tel. +54 (342) 4534451; Fax +54 (342) 4553439; email: mussati@ceride.gov.ar

Received 30 September 2008; Accepted in revised form 5 October 2009

ABSTRACT

This work addresses a flexibility study on a multi-stage flash (MSF) desalination plant. When any plant is designed, the engineers define the design for reaching optimal operation under nominal conditions. However, uncertain variables or disturbance cannot be handled to obtain those nominal conditions. For this reason, the design contains control elements for compensating the disturbance effects. This compensation is only possible into a region defined by the characteristics of the process and the control elements. When the actual conditions are out of that region, the compensation is not enough, and the plant is not operable. A flexibility study determines the region into which the process is operable. This information can be useful for determining design modifications to improve the process flexibility. A flexibility study involves a complex mathematical model, which is even more complex for a MSF plant. To perform the task, in this work, a stationary simulator was developed for a real-world case study, and the region exploration was performed by Monte Carlo simulation. Results show, in terms of both robustness and speed of computation, that this approach can be a useful tool.

Keywords: Flexibility; Simulation; Monte Carlo; MSF

1. Introduction

Traditionally, processes and controllers are designed sequentially. Firstly, the process configurations (structures) and parameters are designed to satisfy the economic objectives, such as maximum profits or minimum operational costs. The designs are based on steady state models, and subjected to the operational constraints. Afterwards, the controllers are designed to reject the likely effects of external disturbances and process uncertainties, as well to achieve the desired dynamic performance. This approach carries a risk in that it may end up choosing the cheapest process design that was difficult to control.

It may also miss out a slightly less economic but easier to control designs, the one that might be more profitable in a long run [1].

Operability properties of a process determine how process dynamics affect the quality of a process control design. These include flexibility, controllability, optimality, stability, selection of measurements and manipulated variables. The flexibility is defined as ‘the ability to maintain the process variables within feasible operational region, despite the presence of uncertainties’ [2]. Flexibility is often considered simultaneously with the economic objectives, hence raises the optimality issue. Therefore, flexibility studies are dominated by numerous optimization strategies. Those studies aim at the determination of flexible operational spaces and flexibility measurements.

* Corresponding author.

The analysis generally involves two complementary tasks, which are the calculation of flexibility index and the flexibility test.

Operational flexibility is an important consideration when designing and operating a chemical plant. Very often, flexibility is concerned with the problem of insuring feasible steady-state operation over a variety of operating uncertainties. To quantify how flexible a process is, various metrics have been developed. Grossmann et al. [2] first introduced the flexibility index *FIG* which quantifies the smallest percentage of the uncertain parameters' expected deviation that the process can handle. Another metric named resilience index *RI* was adopted by Saboo et al. [3]. These two measurements require identification of the nominal point, which must be located within the feasible region. In addition, these measurements just consider the critical uncertainty. This may cause serious flexibility under-estimation or neglect the ability of the process to handle other process uncertainties. To solve this problem, Pistikopoulos and Mazzuchi [4] proposed the stochastic flexibility *SF*. Although *SF* accounts for the chance that the process can operate feasibly, the probability distribution of all the uncertain parameters may not be available at the design stage. Even though the probability distributions are obtainable, the calculation of *SF* is usually tedious. To avoid this difficulty, another index considers the size of the feasible space in which the uncertain parameters can be feasibly handled; this index *FIV* is defined as the size ratio of the feasible space to the overall space bounded by the uncertain parameters' expected limits [5]. The cited indexes, except *FIG* and *RI*, belong to the interval [0, 1], and a higher value means a higher flexibility.

This paper estimates several flexibility indexes for a multi-stage flash (MSF) desalination plant. This study involves a complex mathematical model. To perform the task, in this work, a stationary simulator was developed, and the region exploration was performed by Monte Carlo simulation [6, 7]. Results show, in terms of both robustness and speed of computation, that this approach can be a useful tool.

2. Flexibility study strategy

The flexibility study strategy proposed in this work will be presented by using the system shown in Fig. 1. In that system, stream F_1 , water at 25°C, and stream F_2 , water at 80°C, are mixed to yield a new stream at 52°C. The pressure at the V_1 input is 1.115×10^5 Pa. The volumetric flow of F_2 is 0.02 m³/s. The tank is open and discharges into the atmosphere; its diameter is 1.5 m and the maximum allowed liquid level is 2 m. The controller CT (a P+I controller) is for controlling the tank temperature, and the controller CL (a P controller) is for controlling the tank level; the respective set points are 52°C and 1 m.

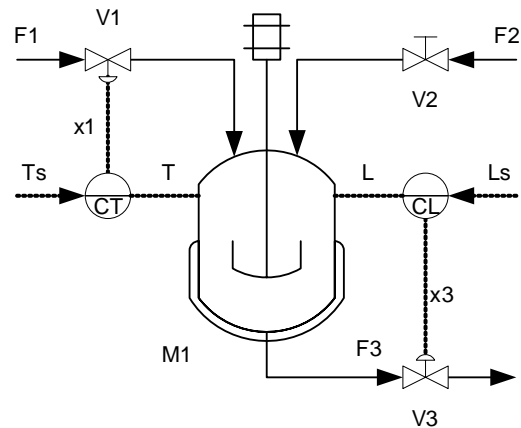


Fig. 1. Mixing tank.

The dynamic model for the mixing tank is conformed by the following equations:

$$\frac{dL}{dt} = \frac{F_1 + F_2 - F_3}{A} \quad (1)$$

$$\frac{dT}{dt} = \frac{F_1(T_1 - T) + F_2(T_2 - T)}{AL} \quad (2)$$

$$\frac{dAi_T}{dt} = e_T \quad (3)$$

$$e_T = T - T_{sp} \quad (4)$$

$$x_1 = Ab_T + K_T \left(e_T + \frac{1}{\tau_{i_T}} Ai_T \right) \quad (5)$$

$$e_L = L - L_{sp} \quad (6)$$

$$x_3 = Ab_L + K_L e_L \quad (7)$$

$$F_1 = C_{v1} x_1 \sqrt{P_1 - P_0} \quad (8)$$

$$F_3 = C_{v3} x_3 \sqrt{\rho g L} \quad (9)$$

where the parameters of controller CT are $T_{sp} = 52^\circ\text{C}$, $Ab_T = 0.5$, $K_T = 0.05^\circ\text{C}^{-1}$ and $\tau_{i_T} = 30$ s; the parameters of controller CL are $L_{sp} = 1$ m, $Ab_L = 0.5$ and $K_L = 20$ m⁻¹. The valves parameters are $C_{v1} = 4.039 \times 10^{-4}$ m^{3.5}/kg^{0.5} and $C_{v3} = 8.078 \times 10^{-4}$ m^{3.5}/kg^{0.5}.

The steady model is obtained from the dynamic one by setting to zero all the derivative terms. The resulting model contains 9 equations and 9 unknowns (F_1 , F_3 , T , L , e_T , x_1 , e_L , x_3 and Ai_T). By removing T , e_T , e_L and Ai_T the

model can be solved by evaluating the following equations:

$$F_1 = F_2 \frac{(T_2 - T_{sp})}{(T_{sp} - T_1)} \tag{10}$$

$$x_1 = \frac{F_1}{C_{v1} \sqrt{P_1 - P_0}} \tag{11}$$

and by solving the following equation system:

$$F_3 = F_1 + F_2 \tag{12}$$

$$x_3 = \frac{F_3}{C_{v3} \sqrt{\rho g L}} \tag{13}$$

$$x_3 = Ab_L + K_L (L - L_{sp}) \tag{14}$$

3. Standardization of variables

Every variable has to be standardized as follows:

$$\delta X = \frac{X - X_n}{\Delta X_n} \tag{15}$$

where X is the variable’s value, X_n is the nominal value that was considered for the variable during the system design, ΔX_n is the half-band of acceptable variability for the variable. Therefore, δX is a dimensionless value that belongs to the open interval $(-1, 1)$ under normal conditions, taking the null value at the nominal condition.

The study considers two set of variables. The first set, called D , is formed by the disturbances; the second one, called Y , is formed by the other process variables (i.e., all the variables of the process, except disturbances). For the mixing tank, the selected disturbances are F_2 and T_2 ; whereas the selected process variables are x_1 and x_3 .

4. Overall and feasible spaces

According to the above definitions, the overall space bounded by the uncertain parameters’ expected limits [5] can be defined as:

$$|\delta X_j| \leq 1 \quad \forall j \in D \tag{16}$$

On the other hand, the feasible space in which the uncertain parameters can be feasibly handled, and so the process is operable, can be defined as:

$$|\delta X_j| < 1 \quad \forall j \in Y \tag{17}$$

In order to determine whether the process is operable or not for a given point of the overall space, it is convenient define the operability index in the following way:

$$I_o = \max_{j \in Y} (|\delta X_j|) \tag{18}$$

While I_o — the maximum observed deviation for the process variables — belongs to the interval $[0, 1)$, the process is operable for the present conditions because the deviations of all process variables are less than the respective acceptable variabilities. This index is used to determine the feasible space, in which the uncertain parameters can be feasibly handled: the feasible space is conformed by all the process states with I_o belonging to the interval $[0, 1)$.

Fig. 2 presents the overall space for two disturbances. A square defined by the inscribing circle with radius r and center $(0, 0)$ is also shown in that figure; that square is called the maximum square if it is the largest square that can be defining into the feasible space.

The probability of the disturbances yield a point into the maximum square depends on the probability distributions associated with the disturbances. If every disturbance follows the uniform distribution (Fig. 3), that probability has the distribution presented in Fig. 4. Conversely, if every disturbance follows the triangular distribution (Fig. 5), that probability has the distribution presented in Fig. 6. Both distribution (Fig. 4 and Fig. 6) were obtained by Monte Carlo simulation with a sample of 1000 points [6,7].

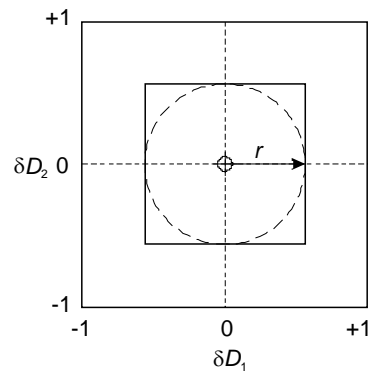


Fig. 2. Overall space for two disturbances.

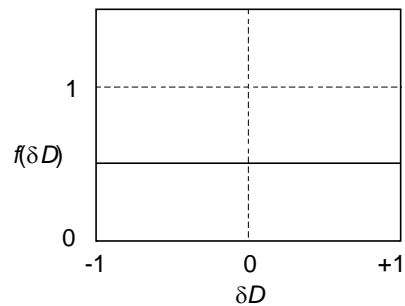


Fig. 3. Uniform distribution for δD .

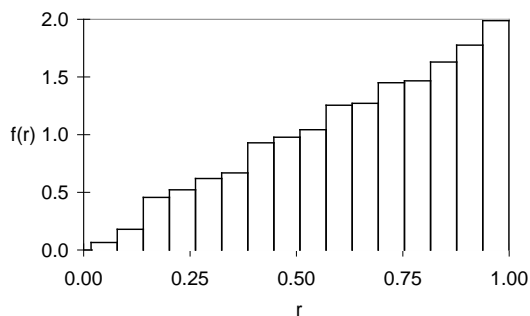


Fig. 4. Probability distribution of r for uniform distribution of δD . The mean is 0.66.

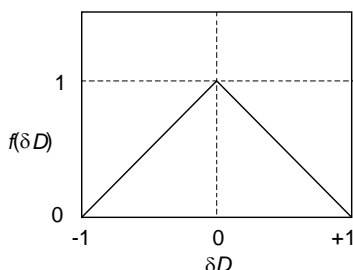


Fig. 5. Triangular distribution for δD .

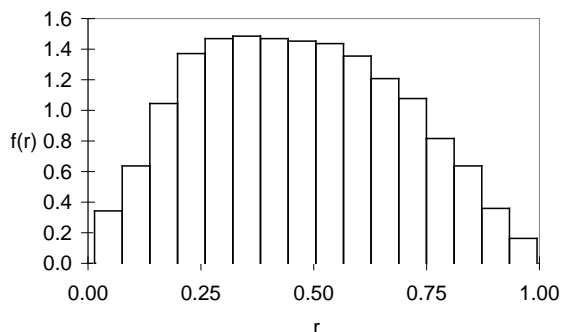


Fig. 6. Probability distribution of r for triangular distribution of δD . The mean is 0.47.

For those particular distributions, it is possible determine analytically the respective probability density function -pdf- $f(r)$ and the cumulative distribution function -cdf- $F(r)$ [8] associated to the maximum hypercube of dimension n (maximum square if $n = 2$). If every disturbance follows the uniform distribution, the corresponding pdf and cdf for the maximum hypercube of dimension n are:

$$f(r) = nr^{n-1} \tag{19}$$

$$F(r) = r^n \tag{20}$$

If every disturbance follows the triangular distribution, the corresponding pdf and cdf for the maximum hypercube of dimension n are:

$$f(r) = 2n(r^2 + 2r(1-r))^{n-1}(1-r) \tag{21}$$

$$F(r) = (r^2 + 2r(1-r))^n \tag{22}$$

Then, the probability of the combination of disturbances be constrained to the maximum square defined by r is equal to $\int_0^r F(t) dt$.

The maximum hypercube is useful because it is easy to verify whether a given operating point is into it, which is a sufficient condition to guarantee the process operability. If the point is outside the maximum square, a deeper analysis is needed such as the outlined below.

5. Flexibility study for the mixing tank

Table 1 presents the nominal values and half-bands of variability adopted for the mixing tank. Fig. 7 shows the corresponding feasible space (without shadow). According to that figure, the process is not operable for T_2 below 52°C (the set point value for the controller CT), a constant limit; however, the upper limit for T_2 is a function of F_2 . The radius r of the inscribing circle into the maximum square is equal to 0.42. By using the corresponding cdf, it can be estimated the maximum square covers 18% of the possible cases if every disturbance has uniform dis-

Table 1
Nominal values and half-bands of acceptable variability for the mixing tank

	F_2 (m ³ /s)	T_2 (°C)	x_1	x_3
Xn	0.02	80	0.5	0.5
DXn	0.01	40	0.5	0.5

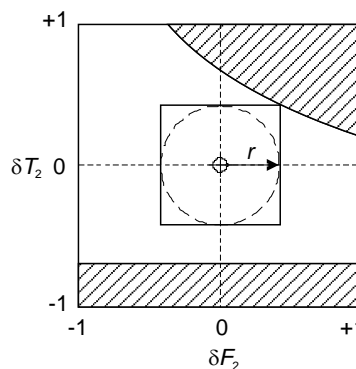


Fig. 7. Feasible space (without shadow) for the mixing tank, $r = 0.42$.

tribution; whereas the covered cases are 44% when every disturbance follows the triangular distribution.

Fig. 8 presents the values adopted by the process variables into the feasible space. Several simulations were run to obtain that figure. In each simulation, a particular combination of disturbances was generated, and the corresponding values for the process variables were also calculated. If the process state thus obtained belonged to the feasible space — i.e., with l_0 belonging to the interval $[0, 1)$ —, the pair δx_1 and δx_3 was added to the plot as the pair n . The most critical variable is x_1 because it reaches the limits of acceptable variability; therefore, the feasible space can be expanded by acting on the sector supervised by the controller CT (e.g., increasing the size of valve V1 or decreasing temperature T_1). In fact, from Eq. (11) it is evident that it is possible to reduce x_1 (the critical variable) by just increasing C_{v1} (i.e., the size of valve V1) without change the other variables. From Fig. 8, it can be deduced that the reduction of x_1 will cause that some process states become now feasible states, increasing in this way the feasible space. That is one of the several conclusions that can be obtained from that figure, and that it is just one advantage of the proposed method. To prove that the previous conclusion is correct, that was tested out by determining the new feasible space when C_{v1} is multiplied by two. The new feasible space thus obtained is bigger than the original one. Again, the same conclusion was obtained, but it required many simulations. That fact remarks the utility of the information presented by Fig. 8, which is a contribution of the proposed method.

Fig. 9 shows process states corresponding to representative points of the overall space. That figure is a representation of parallel coordinates; which is a common way of visualizing high-dimensional geometry and analyzing multivariate data. To show a set of points in an n -dimensional space, a backdrop is drawn consisting of n parallel lines, typically vertical and equally spaced. A point in n -dimensional space is represented as a poly-line with vertices on the parallel axes; the position of the vertex on the i -th axis corresponds to the i -th coordinate of the point. In this work, the set of represented points correspond to the studied process states — i.e., every plotted polyline represents a particular steady state— while the axis represent to the studied variable — e.g., Fig. 9 has axis for F_2, T_2, x_1 and x_3 . In Fig. 9, every point of the overall space is depicted by a line linking the values corresponding to all the considered δX . Of those points, only those with absolute values of δx_1 and δx_3 lesser than 1 are operable —i.e., those process states belong to the feasible space. That figure also shows that x_1 is the most critical variable; moreover, the strong effect of T_2 over x_1 is evident, being a decreasing of T_2 more risky than an increasing. Indeed, x_1 is the most critical variable because it is the variable with most values out of interval $(-1, 1)$. The effect of T_2 on x_1 provokes that the polylines associated to an increase of T_2 are also associated to an increase

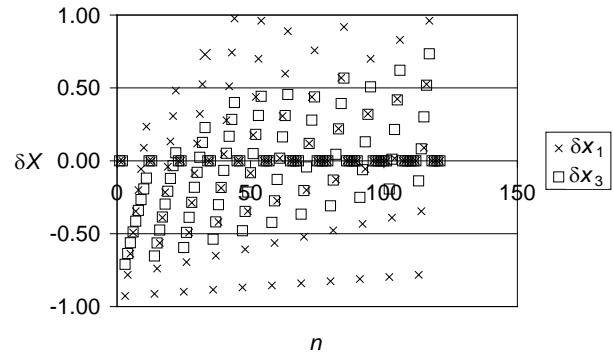


Fig. 8. Process variables in the feasible space for the mixing tank.

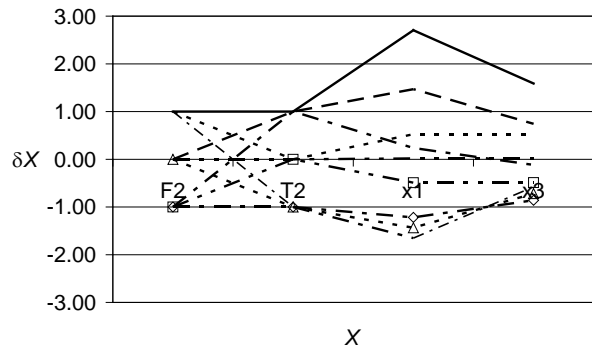


Fig. 9. Representative points of the overall space.

of x_1 ; the equivalent relation exist between the decrease of T_2 and the decrease of x_2 , but it is weaker. This result is just one of all that can be obtained from those figures, and it is another contribution of the proposed method.

6. Flexibility indexes

Different kinds of indexes were defined trying to represent the process flexibility. In general, the better is the index; the more complex is its calculation. That is why, at the first design stages, the simpler indexes can be used; but for the last design stages or for processes already in operation, it is convenient to employ the most exact indexes. For this reason, several indexes were evaluated for the mixing tank. Those indexes are presented below ordered by increasing quality and complexity.

The first index is Iv (it is equivalent to FIG [2] while $FIG \leq 1$) that is defined as:

$$Iv = r \tag{23}$$

where r is the radius of the inscribing circle into the maximum square.

The second index is Ic , which is defined as the size ratio of the maximum hypercube of dimension n (maximum square if $n = 2$) to the overall space:

$$I_c = r^n \tag{24}$$

The third index is I_r , which is defined as the size ratio of the feasible space to the overall space (it is equivalent to FIV [5]). All the above indexes belong to the interval $[0, 1]$, and the value 1 represents the maximum flexibility.

The three introduced indexes are conservative because they take into account a subspace (i.e., the maximum square or hypercube) of the whole feasible space. Besides, those indexes rely on geometric ratios between the feasible space and the overall space, which is adequate when every disturbance follows the uniform distribution. However, for other distributions, it is necessary to define additional indexes; thus, the fourth defined index is P_c , the probability of the disturbances yield a point into the maximum square (or hypercube), which depends on the probability distributions associated with the disturbances. Eqs. (20) and (22) are used to calculate P_c for uniform and triangular distributions respectively; for other distributions, Monte Carlo simulation can be utilized for that proposal [6,7]. The fifth and last index is P_r , the probability of the disturbances yield a point into the feasible space (it is equivalent to SF [4]), which also depends on the probability distributions associated with the disturbances and it is the index most difficult to calculate. In this work, that index was calculated by Monte Carlo simulation with 10000 samples. Table 2 shows all the defined indexes calculated for the mixing tank. In the calculation, it was assumed triangular distribution for the disturbances. If the disturbances yield a point into the feasible space, the process is operable in those conditions by definition. Therefore, the more the probability of the disturbances yield a point into the feasible space, the more the probability of the process is operable – i.e., the process is more flexible. From all the indexes presented in Table 2, the more realistic and useful is P_r , which represents the probability that the process be

Table 2
Flexibility indexes for the mixing tank

I_v	I_c	I_r	P_c	P_r
0.42	0.18	0.68	0.44	0.88

operable. The value 0.88 may be enough for somebody; if not, the modifications suggested by studying Fig. 8 and Fig. 9 can be implemented to expand the feasible space, and thus increases P_r . That analysis is an important part of the proposed strategy.

7. MSF modeling

The strategy proposed to perform a flexibility study was applied to analyze a MSF desalination plant (Fig. 10), which has a series of flash units (stages) where sea water is evaporated to obtain distilled water [9]. The plant has N stages; the first M ones belong to the recovery section, whereas the remaining ones belong to the rejection section. There are also six P+I controllers, which enable to set the operating conditions for the heater, the feed, the recycle and the last stage level.

In this work, the process dynamic model consists of a set of ordinary differential equations and a set of algebraic equations developed by Tarifa and Scenna [9]. The steady model was obtained by setting to 0 every derivative term. The model parameters were set to represent the system studied by Thomas et al. [10]. This system has 15 stages in the recovery section and 3 stages in the rejection section. Table 3 shows the adopted operating condition.

8. Flexibility study for the MSF plant

On one hand, the disturbances to consider in this work are the seawater temperature T_{sw} and the seawater salin-

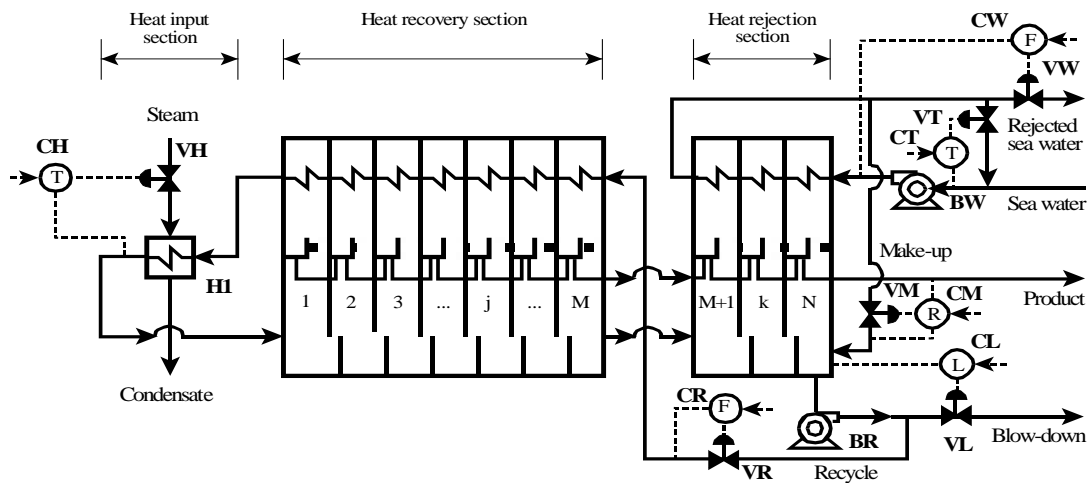


Fig. 10. The MSF system.

Table 3
Operating conditions

Seawater:
$T_{sw} = 28^\circ\text{C}$
$X_{sw} = 51500 \text{ ppm}$
Vapour:
$P_{vh} = 0.937 \text{ atm}$
Controller set points:
$T_{0s} = 90^\circ\text{C}$
$L_s = 0.6 \text{ m}$
$W_{cws} = 14800 \text{ tn/h}$
$T_{cws} = 33^\circ\text{C}$
$R_{mus} = 4.6$
$W_{bs} = 14380 \text{ tn/h}$

ity X_{sw} . Those variables show a wide range of variability, and they have large effects on MSF plants operation [11]. On the other hand, the process variables to consider in the study are presented in Table 4.

Table 5 presents the nominal values and half-bands of variability adopted for the MSF plant. For each process variable, its half-band of variability ΔX_n was set equal to 80% of the corresponding nominal value X_n .

Fig. 11 shows the feasible space (without shadow) for the MSF plant. That feasible space was obtained by simulation, which is quite time consuming due to the model complexity. The simulations were performed taking sample with steps equal to 0.20 for δX_{sw} and δT_{sw} . The radius r of the inscribing circle into the maximum square is equal to 0.40. According to the simulations, the process is not operable for T_{sw} above 33°C (the set point T_{cws} value for the controller CT), a constant limit; however, the lower limit for T_{sw} is a function of X_{sw} . That upper limit of T_{sw} corresponds to a value of r equal to 0.60; therefore, the actual radius belongs to the interval

Table 4
Process variables to consider

AL : output of CL.
AW_{mu} : output of CM.
AT_0 : output of CH.
AT_{cw} : output of CT.
AW_b : output of CR.
AW_{cw} : output of CW.

Table 5
Nominal values and half-bands of acceptable variability for the MSF plant

	$T_{sw} (^\circ\text{C})$	X_{sw}	AL	AW_{mu}	AT_0	AT_{cw}	AW_b	AW_{cw}
X_n	30	0.0515	0.35	0.42	0.54	0.32	0.53	0.22
ΔX_n	5	0.0165	0.28	0.34	0.43	0.26	0.42	0.18

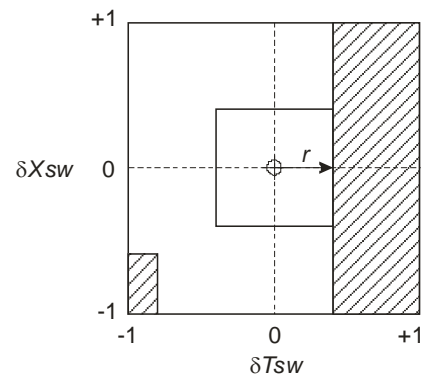


Fig. 11. Feasible space (without shadow) for the MSF plant, $r = 0.40$.

[0.40, 0.6). Taking the worst case, r results equal to 0.40. By using the corresponding cfd, it can be estimated the maximum square covers 16% of the possible cases if every disturbance has uniform distribution; whereas the covered cases are 41% when every disturbance follows the triangular distribution.

Fig. 12 presents the values adopted by some of the analyzed process variables into the feasible space; the remaining ones were not plotted because their changes were not so important. The most critical variable are AT_{cw} and AW_{cw} because they reach the limits of acceptable variability; therefore, the feasible space can be expanded by acting on the sectors supervised by the controllers CT and CW (e.g., increasing the size of corresponding valves).

Fig. 13 shows representative points of the overall space for the MSF plant. Every point is depicted by a line

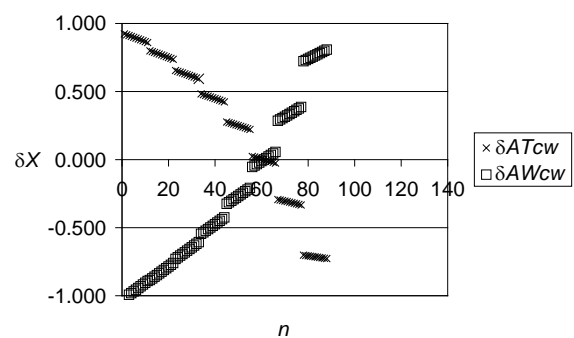


Fig. 12. Process variables in the feasible space for the MSF plant.

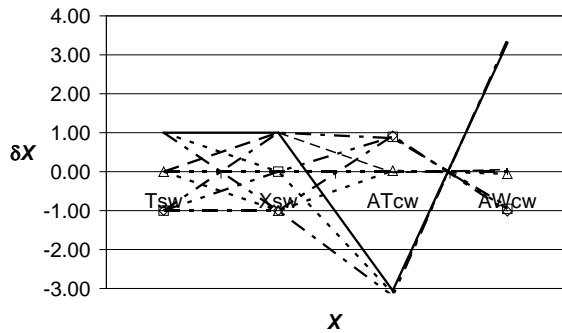


Fig. 13. Representative points of the overall space.

linking the values corresponding to all the considered δX . Of those points, only those with absolute values of δAT_{cw} and δAW_{cw} lesser than 1 are operable. That figure also shows that both process variables, AT_{cw} and AW_{cw} , are critical; moreover, the strong effect of T_{sw} on them is evident, being an increasing of T_{sw} more risky than a decreasing.

Finally, Table 6 shows the previously defined indexes calculated for the MSF plant. In the calculation, it was again assumed triangular distribution for the disturbances.

Table 6
Flexibility indexes for the MSF plant

I_v	I_c	I_r	P_c	P_r
0.40	0.16	0.68	0.41	0.82

9. Conclusion

A strategy to perform a flexibility study was presented and it was applied to a MSF plant. The strategy begins with a steady model of the analyzed process. Next, the main disturbances and process variables are identified. Those variables are then properly standardized. The feasible space is determined by simulation. At this point, a set of indexes can be evaluated and, in this manner, the process flexibility is estimated.

The proposed study enables to determine the probability associated to the feasible space. Besides, the study enables to identify the critical variables of the process; thus, the flexibility can be increased by acting on them. The inverse problem can also be considered, i.e., determining the effects on the process flexibility produced by a modification into the plant. Then, the new feasible space, its new associated probability and the involved costs will establish together the convenience of that modification.

Symbols

τI	Integral time constant, s
δX	Standardized variables
ΔX_n	Half-bands of acceptable variability
A	Cross sectional area, m^2
A_b	Controller bias
A_i	Integral effect of CT, $s \times ^\circ C$
AL	Output of CL
AT_0	Output of CH
AT_{cw}	Output of CT
AW_b	Output of CR
AW_{cw}	Output of CW
AW_{mu}	Output of CM
C_v	Valve flow coefficient, $m^{3.5}/kg^{0.5}$
D	Disturbances
D	Set of disturbances
e_L	Controller error of CL, m
e_T	Controller error of CT, $^\circ C$
F	Volumetric flow, m^3/s
I_o	Operability index
I_v, I_c, I_r	Flexibility indexes
j	Variables (subscript)
K_L	Gain of CT, $^\circ C^{-1}$
K_T	Gain of CT, m^{-1}
L	Level, m
L_s	Set point of CL for the MSF system, m
L_{sp}	Set point of CL for the mixing tank, m
M	Number of stages in the recovery section of the MSF plant
N	Total stages of the MSF plant
P	Pressure, atm
P_c, P_r	Probabilities
P_{vh}	Heater vapour pressure, atm
r	Radius of the inscribing circle into the maximum square
R_{mu}	Set point of CM
T	Temperature, $^\circ C$
t	Time, s
T_0s	Set point of the CH, $^\circ C$
T_{cws}	Set point of CT for the MSF system, $^\circ C$
T_{sp}	Set point of the CT for the mixing tank, $^\circ C$
T_{sw}	Seawater temperature, $^\circ C$
x	Valve opening
X	Variables
X_n	Nominal values
X_{sw}	Seawater salt mass fraction
Y	Set of process variables
W_b	Set point of CR, tn/h
W_{cws}	Set point of CW, tn/h

Acknowledgement

The authors wish to acknowledge the financial support of the Consejo Nacional de Investigaciones Cientí-

ficas y Técnicas CONICET (Argentina) and Universidad Nacional de Jujuy UNJu (Argentina).

References

- [1] O. Weitz and D.R. Lewin, Dynamic controllability and resiliency diagnosis using steady state process flowsheet data, *Comp. Chem. Eng.*, 20(4) (1996) 325–335.
- [2] I.E. Grossmann, K.P. Halemane and R.E. Swaney, Optimization strategies for flexible chemical processes, *Comp. Chem. Eng.*, 7(4) (1983) 439–462.
- [3] A.K. Saboo, M. Morari and D.C. Woodcock, Design of resilient processing plants. VIII: A resilience index for heat exchanger networks, *Chem. Eng. Sci.*, 40(8) (1985) 1553–1565.
- [4] E.N. Pistikopoulos and T.A. Mazzucchi, A novel flexibility analysis approach for processes with stochastic parameters, *Comp. Chem. Eng.*, 14(9) (1990) 991–1000.
- [5] S.-M. Lai and C.-W. Hui, Measurement of plant flexibility, *Comp. Aided Chem. Eng.*, 24 (2007) 189–194.
- [6] N. Metropolis and S. Ulam, The Monte Carlo method, *J. Amer. Stat. Assoc.*, 44 (1949) 335–341.
- [7] R.Y. Rubinstein and D.P. Kroese, *Simulation and the Monte Carlo Method*, 2nd ed., John Wiley & Sons, New York, 2007.
- [8] C. Rose and M.D. Smith, *Mathematical Statistics with Mathematics*, Springer-Verlag, New York, 2002.
- [9] E.E. Tarifa and N.J. Scenna, A dynamic simulator for MSF plants, *Desalination*, 138 (2001) 349–364.
- [10] P.J. Thomas, S. Bhattacharyya, A. Patra and G.P. Rao, Steady state and dynamic simulation of multi-stage flash desalination plants: A case study, *Comp. Chem. Eng.*, 22 (10) (1998) 1515–1529.
- [11] M.S. Tanvira and I.M. Mujtaba, Neural network based correlations for estimating temperature elevation for seawater in MSF desalination process, *Desalination*, 195 (2006) 251–272.